SOME OBSERVATIONS REGARDING INTERPOLANTS IN THE LIMIT OF FLAT RADIAL BASIS FUNCTIONS

BENGT FORNBERG*, GRADY WRIGHT†, AND ELISABETH LARSSON‡

Abstract. Radial basis functions (RBFs) form a primary tool for multivariate interpolation. Some of the most commonly used radial functions feature a shape parameter, allowing them to vary from being nearly flat (ε small) to sharply peaked (ε large). The former limit can be particularly accurate when interpolating a smooth function based on scattered data. This study discusses theoretical and computational aspects of the $\varepsilon \to 0$ limit, and includes the conjecture that Gaussian RBF interpolants will never diverge in this limit.

Key words. Radial basis functions, RBF, multivariate interpolation.

AMS subject classifications. 41A10, 41A63, 41A58, 65D05, 65F22, 65F40

1. Introduction. When collocating n pieces of data in one dimension, one first chooses some set of basis functions $\psi_k(x)$, and then determines expansion coefficients λ_k such that the linear combination

$$s(x) = \sum_{k=1}^{n} \lambda_k \psi_k(x)$$

satisfies all the constraints. For many choices of $\psi_k(x)$, interpolation is guaranteed to be non-singular whenever the data points are distinct. With certain point distributions, it may furthermore be possible to choose basis functions that possess some orthogonality properties, e.g., Fourier modes on a periodic interval, or Chebyshev polynomials on a finite interval. In more than one dimension, the situation is very different. There no longer exist any basis functions $\psi_k(\underline{x})$ so that non-singularity for interpolation can be guaranteed for more than $n = 1$ data point [1]. The RBF approach circumvents this problem by following a somewhat different strategy. Instead of using a sequence of (typically increasingly oscillatory) basis functions that are independent of the data point locations $\underline{x}_k$, one uses instead translates of one single non-oscillatory function $\phi(\|\underline{x}\|)$:

$$s(\underline{x}) = \sum_{k=1}^{n} \lambda_k \phi(\|\underline{x} - \underline{x}_k\|) \ , \tag{1.1}$$

where $\|\cdot\|$ is the standard Euclidean vector norm. Table 1.1 shows a few of the many choices available for $\phi(r)$. Existence and uniqueness of the interpolants $s(\underline{x})$ are discussed for example in [2, 3, 4]. For all three choices of smooth basis functions listed (IQ, GA, MQ), these are ensured for arbitrary point distributions. To ensure these for the piecewise smooth basis functions listed, (1.1) may require some modifications [2].

Type of basis function	$\phi(r)$
Piecewise smooth RBFs	
Piecewise polynomial (R_n)	$|r|^n$, n odd
Thin Plate Spline (TPS_n)	$|r|^n \ln r$, n even
Infinitely smooth RBFs	
Multiquadric (MQ)	$\sqrt{1 + (\varepsilon r)^2}$
Inverse quadratic (IQ)	$\frac{1}{1+(\varepsilon r)^2}$
Gaussian (GA)	$e^{-(\varepsilon r)^2}$

TABLE 1.1
Some commonly used radial basis functions

The piecewise smooth $\phi(r)$, such as cubics and TPS will, as the number of data points is increased, give an algebraic rate of convergence (to a smooth function). The rate reflects the severity of the irregularity of $\phi(r)$ at the origin, and it typically increases with the number of space dimensions [5]. In contrast to this, the infinitely smooth RBFs often lead to spectral convergence (when proper attention is paid to boundary effects), i.e. $O(e^{-\text{const.}/h})$ (or $O(e^{-\text{const.}/h^2})$ in case of GA RBFs) where h is a 'typical' distance between neighboring data locations [6, 7, 8].

The value of the shape parameter ε in the smooth RBFs will influence the constants in this estimate. Many studies have been devoted to experimentally establishing suitable values of ε for different situations [9, 10, 11]. Although small but non-zero values of ε usually are optimal, the limit of flat radial functions ($\varepsilon \to 0$) has recently been found to have a number of intriguing features:

- For arbitrarily spaced data in 1-D, the limiting interpolant usually agrees with Lagrange's interpolation polynomial [12]. In higher-D, the limiting interpolant (when it exists) will again be a low degree multivariate polynomial. This means that RBFs can be a tool for generalizing, to irregular grids and domains, the 'classical' spectral methods (which typically are based on 1-D high-order polynomial interpolants, cf. [13]).
- Small values of ε have been found to yield very accurate results when interpolating smooth functions [14], solving elliptic PDEs with RBFs [15], and approximating data on low-dimensional manifolds within high-dimensional spaces [16].
- The direct method of solving for the RBF interpolant via the expansion coefficients λ_k in (1.1) becomes extremely ill-conditioned as $\varepsilon \to 0$ [7]. However, recently a numerically stable algorithm has been found that largely overcomes this ill-conditioning problem and allows for the stable computation of the RBF interpolants for the full range of ε [14]. Although the present algorithm appears to be limited to relatively small data sets, it still demonstrates that the ill conditioning is not in any way intrinsic to RBF interpolation, but only an artifact of certain implementations. A perfectly stable algorithm for any number of points may very well be feasible. In any case, RBF interpolants based on up to around 100 data points (in 2-D; more in higher-D) can at present be explored numerically for all values of ε, including in the limit of $\varepsilon \to 0$.

In very special cases divergence can occur when $\varepsilon \to 0$, as was first noted in [12] for a case when all the data points were given on a finite Cartesian grid. However, for randomly scattered data, there has never been found an instance in which the RBF

interpolant fails to exist in the limit of $\varepsilon \to 0$. One of the goals of this paper is to try to shed more light on the nature of such exceptional situations. One key tool for that is the simple closed-form expression for the RBF interpolant to cardinal data (equal to one at one node point, and zero at the others) that is given in Section 2. This formula is used to determine the interpolants in the examples in Section 3. These examples cause us to become particularly interested in the Gaussian (GA) RBFs, for which we formulate a conjecture. In Section 4, we relate the observed features of RBF interpolants to those of multivariate interpolation polynomials. We also summarize some new theoretical results regarding limiting interpolants for scattered data, which will be presented in more detail separately [17]. Although we primarily are interested in real values of ε, considering complex values of ε not only provides additional insights, but also leads to the only computational algorithm that is available for $\varepsilon \to 0$ studies [14]. In Section 5, we very briefly review this algorithm, and we then use it to re-visit and extend some of the examples from Section 3. An often considered variation of (1.1) is $s(\underline{x}) = \alpha + \sum_{k=1}^{n} \lambda_k \phi(\|\underline{x} - \underline{x}_k\|)$ together with the constraint $\sum_{k=1}^{n} \lambda_k = 0$. Our brief study of this in Section 6 does not suggest that it offers any particular advantages in the limit of $\varepsilon \to 0$. The final Section 7 contains some concluding remarks.

2. Closed-form expression for the RBF interpolant. With data values f_k at locations $\underline{x}_k$, $k = 1, 2, \ldots, n$, the RBF interpolant becomes

$$s(\underline{x}) = \sum_{k=1}^{n} \lambda_k \, \phi\left(\|\underline{x} - \underline{x}_k\|\right) \ . \tag{2.1}$$

The coefficients λ_k can be obtained by solving the linear system

$$\begin{bmatrix} & & \\ & A & \\ & & \end{bmatrix} \begin{bmatrix} \lambda_1 \\ \vdots \\ \lambda_n \end{bmatrix} = \begin{bmatrix} f_1 \\ \vdots \\ f_n \end{bmatrix} , \tag{2.2}$$

where the entries of the matrix A are $A_{i,j} = \phi\left(\|\underline{x}_i - \underline{x}_j\|\right), i = 1, \ldots, n, \ , j = 1, \ldots, n$. As mentioned in the introduction, this linear system is guaranteed to be non-singular for the IQ, GA, and MQ RBFs (assuming the data locations are unique). For some other choices of $\phi(r)$, it may be necessary to augment (2.1) with some low order polynomial terms and additional constraints in order to guarantee that (2.2) is non-singular (see for example [2]).

THEOREM 2.1. *For cardinal data* $f_k = \begin{cases} 1 & \text{if } k = 1 \\ 0 & \text{otherwise} \end{cases}$ *, the RBF interpolant of the form (2.1) becomes*

$$s(\underline{x}) = \frac{\det \begin{bmatrix} \phi(\|\underline{x} - \underline{x}_1\|) & \phi(\|\underline{x} - \underline{x}_2\|) & \cdots & \phi(\|\underline{x} - \underline{x}_n\|) \\ \phi(\|\underline{x}_2 - \underline{x}_1\|) & \phi(\|\underline{x}_2 - \underline{x}_2\|) & \cdots & \phi(\|\underline{x}_2 - \underline{x}_n\|) \\ \vdots & \vdots & \ddots & \vdots \\ \phi(\|\underline{x}_n - \underline{x}_1\|) & \phi(\|\underline{x}_n - \underline{x}_2\|) & \cdots & \phi(\|\underline{x}_n - \underline{x}_n\|) \end{bmatrix}}{\det \begin{bmatrix} \phi(\|\underline{x}_1 - \underline{x}_1\|) & \phi(\|\underline{x}_1 - \underline{x}_2\|) & \cdots & \phi(\|\underline{x}_1 - \underline{x}_n\|) \\ \phi(\|\underline{x}_2 - \underline{x}_1\|) & \phi(\|\underline{x}_2 - \underline{x}_2\|) & \cdots & \phi(\|\underline{x}_2 - \underline{x}_n\|) \\ \vdots & \vdots & \ddots & \vdots \\ \phi(\|\underline{x}_n - \underline{x}_1\|) & \phi(\|\underline{x}_n - \underline{x}_2\|) & \cdots & \phi(\|\underline{x}_n - \underline{x}_n\|) \end{bmatrix}} \tag{2.3}$$

Proof. Solving (2.2) by Cramer's rule and substituting into (2.1) leads, in just a few lines of algebra, to (2.3). However, the easiest demonstration is probably by inspection. By expanding the determinant in the numerator along its first row, we see that the expression for $s(\underline{x})$ indeed becomes of the form of (2.1). Furthermore, it will evaluate to one for $\underline{x} = \underline{x}_1$ (since then the two determinants become equal) and to zero for $\underline{x} = \underline{x}_k, k \neq 1$ (since then two rows in the determinant in the numerator become equal). □

One immediate consequence of this result is the following:

THEOREM 2.2. *If* $\lim_{\varepsilon \to 0} s(\underline{x})$ *exists, it will be a (multivariate) finite degree polynomial in* $\underline{x}$.

Proof. If we expand $\phi(\|\underline{x} - \underline{x}_k\|)$ in powers of ε^2, the coefficient for ε^{2m} will be a polynomial of degree (at most) $2m$ in the components of $\underline{x}$. The same will therefore hold for the determinant in the numerator of (2.3), and the ratio in (2.3) will be of the form

$$s(\underline{x}) = \frac{\varepsilon^{2p}\{\text{pol. degree } 2p\} + \varepsilon^{2p+2}\{\text{pol. degree } 2p+2\} + \dots}{\varepsilon^{2q}\{\text{constant}\} + \varepsilon^{2q+2}\{\text{constant}\} + \dots}$$

where p and q are positive integers. Since $s(x_1) = 1$, $p > q$ is impossible. If $p < q$, the limit fails to exist. Otherwise (i.e. when $p = q$) it will become a polynomial of degree (at most) $2p$ in the components of $\underline{x}$.□

Theorem 2.2 appears to have been discovered independently a number of times during the last decade or so. However, we have been unable to locate it in any previous reference. It was however shown in [12] that, in 1-D and subject to some minor constraint on $\phi(r)$, the limit is the lowest order interpolation polynomial, i.e. of degree $n - 1$ in case of n data points (and that, failing these constraints, the limit would still be of polynomial type, but that the degree could be higher). The situation for higher-D can be considerably more complex, as will be discussed below (and analyzed further in [17]).

3. A collection of examples with closed-form solutions for the $\varepsilon \to 0$ **limit.** The first several examples in this section concern the situation when increasingly many points are located along a straight line. In most of these cases, closed-form analysis is possible, offering key insights and motivation for the more general discussion in Section 4 (where we examine polynomial unisolvency and interpolants for scattered points in more dimensions).

3.1. Three points along a straight line: Evaluation along the line. Let the three points be located at $\{x_1, x_2, x_3\}$ and the corresponding data values be $\{1, 0, 0\}$ (The results become equivalent for $\{0, 1, 0\}$ and $\{0, 0, 1\}$ and, since the interpolation procedure is linear, also for arbitrary data). With a radial function

$$\phi(r) = a_0 + a_1(\varepsilon r)^2 + a_2(\varepsilon r)^4 + \dots$$

we get

$$\det \begin{bmatrix} \phi(|x - x_1|) & \phi(|x - x_2|) & \phi(|x - x_3|) \\ \phi(|x_2 - x_1|) & \phi(|x_2 - x_2|) & \phi(|x_2 - x_3|) \\ \phi(|x_3 - x_1|) & \phi(|x_3 - x_2|) & \phi(|x_3 - x_3|) \end{bmatrix} =$$

$$= 2a_1(a_1^2 - 6a_0a_2)(x - x_2)(x - x_3)(x_1 - x_2)(x_1 - x_3)(x_2 - x_3)^2\varepsilon^6 + O(\varepsilon^8)$$

and

$$\det \begin{bmatrix} \phi(|x_1 - x_1|) & \phi(|x_1 - x_2|) & \phi(|x_1 - x_3|) \\ \phi(|x_2 - x_1|) & \phi(|x_2 - x_2|) & \phi(|x_2 - x_3|) \\ \phi(|x_3 - x_1|) & \phi(|x_3 - x_2|) & \phi(|x_3 - x_3|) \end{bmatrix} =$$

$$= 2a_1(a_1^2 - 6a_0a_2)(x_1 - x_2)^2(x_1 - x_3)^2(x_2 - x_3)^2\varepsilon^6 + O(\varepsilon^8).$$

On the assumption that $a_1 \neq 0$ and $a_1^2 - 6a_0a_2 \neq 0$, the ratio becomes

$$s(x) = \frac{(x - x_2)(x - x_3)}{(x_1 - x_2)(x_1 - x_3)} + O(\varepsilon^2),$$

i.e. we have recovered the Lagrange interpolation polynomial. According to the main theorem in [12], the same will be the case for any number of points along a line, as long as certain inequalities hold for the Taylor coefficients a_k of the radial function. The two inequalities encountered here are two of an infinite set that is explicitly given in [12]. Although a firm proof is still lacking, current evidence strongly suggest that all of these are satisfied, for example by MQ, IQ, and GA RBFs. We will in the following assume that these inequalities hold when we refer to this main theorem of [12].

3.2. Three points along a straight line: Evaluation off the line. When evaluating the interpolant in the previous example at a location (x, y), the first determinant becomes

$$\det \begin{bmatrix} \phi(\sqrt{(x - x_1)^2 + y^2}) & \phi(\sqrt{(x - x_2)^2 + y^2}) & \phi(\sqrt{(x - x_3)^2 + y^2}) \\ \phi(|x_2 - x_1|) & \phi(|x_2 - x_2|) & \phi(|x_2 - x_3|) \\ \phi(|x_3 - x_1|) & \phi(|x_3 - x_2|) & \phi(|x_3 - x_3|) \end{bmatrix} =$$

$$= 2a_1\left[(a_1^2 - 6a_0a_2)(x - x_2)(x - x_3) + (a_1^2 - 2a_0a_2)y^2\right] \cdot$$

$$\cdot (x_1 - x_2)(x_1 - x_3)(x_2 - x_3)^2\ \varepsilon^6\ +\ O(\varepsilon^8)$$

producing the interpolant

$$s(x, y) = \frac{(x - x_2)(x - x_3)}{(x_1 - x_2)(x_1 - x_3)} + \frac{a_1^2 - 2a_0a_2}{a_1^2 - 6a_0a_2}\frac{y^2}{(x_1 - x_2)(x_1 - x_3)} + O(\varepsilon^2). \qquad (3.1)$$

For $y = 0$, i.e. along the x-axis, we recover the previous result. However, a y^2-term is now also present, with a coefficient that depends on the choice of RBF. The factor $\frac{a_1^2 - 2a_0a_2}{a_1^2 - 6a_0a_2}$ takes the values $\frac{1}{2}$, $\frac{1}{5}$, and 0 for MQ, IQ, and GA respectively. Thus the $\varepsilon \to 0$ limits are now different for the different RBFs, but they still exist in all cases.

3.3. Three points not on a line. With the three points located at (x_k, y_k), $k = 1, 2, 3$, the ratio of the two determinants becomes

$$s(x, y) = \frac{4a_1^2(2A)(x\ (y_3 - y_2) - y\ (x_3 - x_2) + x_3y_2 - x_2y_3)\ \varepsilon^4 + O(\varepsilon^6)}{4a_1^2(2A)^2\ \varepsilon^4 + O(\varepsilon^6)} \qquad (3.2)$$

where

$$2A = x_2y_1 - x_3y_1 - x_1y_2 + x_3y_2 + x_1y_3 - x_2y_3 \; ,$$

i.e. $|A|$ is the area of the triangle spanned by the three point locations. When the three points are not collinear (i.e. when $A \neq 0$, and also assuming $a_1 \neq 0$), the limiting interpolant will be the plane that fits the data. As the points become increasingly collinear, the tilt of the plane increases without bound. When the points are collinear, both the coefficients for ε^4 in (3.2) vanish, and the $\varepsilon \to 0$ limit will instead follow from the ε^6 coefficients, as described in the two preceding examples. The limit thus behaves discontinuously with respect to the point locations.

3.4. Five or more points along a straight line. It turns out that increasing from three to four points along a line (say, the x-axis) offers no new phenomenon. For five points along a line, the result along the same line (like for any number of points) becomes the Lagrange interpolation polynomial. However, evaluating at a location (x, y) off the x-axis now gives

$$s(x,y) = \frac{4y^2}{(x_1 - x_2)(x_1 - x_3)(x_1 - x_4)(x_1 - x_5)} \cdot$$
$$\cdot \frac{(a_1a_2^2 - 3a_1^2a_3 + 3a_0a_2a_3)}{(6a_2^3 + 225a_0a_3^2 + 70a_1^2a_4 - 30a_1a_2a_3 - 420a_0a_2a_4)} \, \frac{1}{\varepsilon^2} \; + \; O(1) \tag{3.3}$$

(assuming $2a_2^2 - 5a_1a_3 \neq 0$; both this assumption and the denominator above being non-zero belong to the set of inequalities discussed above). The ratio involving the coefficients a_k, $k = 1, \ldots, 4$ in (3.3) takes for MQ, IQ, and GA the values $\frac{1}{28}$, $\frac{1}{149}$ and 0 respectively. If for example $\phi(r) = (1 + (\varepsilon r)^2)^{\beta/2}$ (an 'unconditionally positive definite' case with non-singularity of the interpolant guaranteed for any $\beta < 0$, cf. [2, 3]), the assumption $2a_2^2 - 5a_1a_3 \neq 0$ becomes $\beta \neq 0$, $\beta \neq 2$, $\beta \neq 7$, and the coefficient ratio becomes always non-zero: $-3/(\beta^3 - 19\beta^2 + 99\beta - 165)$, i.e. divergence as $\varepsilon \to 0$.

Increasing to 7, 9, ... points, we typically get divergence like $O(1/\varepsilon^4)$, $O(1/\varepsilon^6)$, etc. For non-divergence, increasingly numerous and intricate requirements on the coefficients a_k need to hold. GA are remarkable in satisfying them all, as follows from the theorem below:

THEOREM 3.1. *With any number of data points along a straight line, GA interpolants will not diverge as $\varepsilon \to 0$ when evaluated anywhere on or off the line.*

Proof. Along the x-axis, (i.e. $y = 0$), the GA interpolant takes the form $s(x, \varepsilon) = \sum_k \lambda_k e^{-\varepsilon^2(x-x_k)^2}$. At (x, y), the value becomes $r(x, y, \varepsilon) = \sum_k \lambda_k e^{-\varepsilon^2((x-x_k)^2 + y^2)} = e^{-\varepsilon^2 y^2} s(x, \varepsilon)$. Both of these factors remain bounded as $\varepsilon \to 0$ (obviously for the first one, and the second one converges to Lagrange's interpolation polynomial, according to the main theorem in [12]). Therefore, the product also remains bounded. ◻

Both numerical and some analytical evidence suggest that certain other RBFs share the property of GA interpolants shown in Theorem 3.1, e.g. $\phi(r) = J_0(\varepsilon r)$ and $\phi(r) = \frac{\sin(\varepsilon r)}{\varepsilon r}$. Since these functions are oscillatory, they have seldom been considered for practical RBF work (with one reason for this being that oscillatory RBFs can never provide non-singular interpolation for all data sets in all dimensions). However, with finite-sized data sets and small ε, the oscillations would never be seen, and it could be that oscillatory radial functions deserve some further considerations.

Dimension of hyperplane: $d =$	1	2	3	4	5	6	7	8
Lowest number of points to feature divergence off the hyperplane; $N_d =$	5	11	21	36	57	85	121	166

TABLE 3.1

Lowest number of scattered data points in a hyperplane to cause divergence off the plane

In the doubly infinite case of $x_k = k$, $k = -\infty, \ldots, -1, 0, 1, \ldots, \infty$, the situation is again different—there is no divergence (as $\varepsilon \to 0$) off the line for any of the smooth RBF choices [18].

3.5. Some generalizations to higher dimensions. The result in Theorem 3.1 can be extended as follows:

THEOREM 3.2. *In the case when the data points are laid out in a finite rectangular lattice (in any number of dimensions), GA interpolants will not diverge as $\varepsilon \to 0$.*

Proof. For notational simplicity, we consider the 2-D case. Let the lattice be $\{x_i, y_j\}$, $i = 1, \ldots m$, $j = 1, \ldots n$. It suffices to show the result for cardinal data, i.e. if for some fixed i and j it holds that

$$f = \left\{ \begin{array}{ll} 1 & \text{when } x = x_i \text{ and } y = y_j \\ 0 & \text{otherwise} \end{array} \right. .$$

Consider the 1-D interpolants

$$r(x, \varepsilon) = \sum_{k=1}^{m} \lambda_k e^{-\varepsilon^2 (x - x_k)^2} \quad \text{satisfying} \quad r(x, \varepsilon) = \left\{ \begin{array}{ll} 1 & x = x_i \\ 0 & \text{otherwise} \end{array} \right.$$

$$s(y, \varepsilon) = \sum_{l=1}^{n} \mu_l e^{-\varepsilon^2 (y - y_l)^2} \quad \text{satisfying} \quad s(y, \varepsilon) = \left\{ \begin{array}{ll} 1 & y = y_j \\ 0 & \text{otherwise} \end{array} \right.$$

The product $r(x, \varepsilon) \cdot s(y, \varepsilon) = \sum_{k=1}^{m} \sum_{l=1}^{n} \lambda_k \mu_l e^{-\varepsilon^2 (x - x_k)^2 - \varepsilon^2 (y - y_l)^2}$ satisfies all that is required of the 2-D GA interpolant, and is therefore identical to it. Since both of the factors $r(x, \varepsilon)$ and $s(y, \varepsilon)$ remain bounded as $\varepsilon \to 0$ (by the main theorem in [12]), so does their product. □

Equation (3.3) showed that, for five points along a line ($d = 1$), divergence typically occurs when the interpolant is evaluated off the line. Similarly, for scattered points in a plane ($d = 2$), eleven points usually leads to divergence when the interpolant is evaluated off that plane. The data in Table 3.1, obtained with the Contour-Padé algorithm described in Section 5, suggests that $N_d - 1 = \binom{d+3}{3}$.

All instances of divergence that we have encountered occur in situations where 'polynomial unisolvency' (to be defined later) fails. Heuristically, this becomes the case when the data points are located in such a way that multivariate polynomial interpolation leaves some low order coefficient(s) completely undetermined. For example, with points only along the x-axis, coefficients for powers of y are undetermined. Similarly, if we place all the points along a section of a parabola, some other low order polynomial coefficients will be undetermined. This is illustrated next.

3.6. Points placed along a parabola. We let the locations for n points be $x_k = \frac{k-1}{n-1}$, $y_k = x_k^2$, $k = 1, 2, \ldots, n$. This leaves a polynomial interpolant undetermined with respect to several low order polynomials, such as $y - x^2$, $x(y - x^2)$, $y(y - x^2)$,

n	2	3	4	5	6	7
Leading power of ε in numerator = leading power in denominator	2	4	8	12	18	24
Value of interpolant at (0,1) MQ	$\frac{1}{2}$	3	$\frac{69}{10}$	$\frac{89}{3}$	$\frac{12253}{176}$	$-\frac{8043}{40}$
IQ	$\frac{1}{2}$	3	$\frac{27}{4}$	$\frac{493}{15}$	$\frac{22575}{272}$	$\frac{6972}{25}$
GA	$\frac{1}{2}$	3	$\frac{20}{3}$	35	$\frac{189}{2}$	462

TABLE 3.2
Values of the interpolant at (0,1) in the example with points on a parabola

etc. With cardinal data (equal to one at the first point and zero at the remaining ones) we get in this case different limits starting when $n = 4$ (one step later than for points along a line). The leading powers of ε in the expansions in the numerator and denominator of (2.3) increase quite rapidly with n. Table 3.2 illustrates that, and also gives the value of the interpolants in the $\varepsilon \to 0$ limit, evaluated at the point (0,1). For $n = 8$, both MQ and IQ feature a numerator starting with ε^{30} and denominator starting with ε^{32}, producing divergence according to $\frac{117649}{23040} \frac{1}{\varepsilon^2} + \frac{72202965}{65536} + O(\varepsilon^2)$ and $\frac{117649}{127080} \frac{1}{\varepsilon^2} + \frac{643338441829}{538310880} + O(\varepsilon^2)$ respectively. The GA interpolant remains bounded; both leading terms are $O(\varepsilon^{32})$, and the limit value is $\frac{6864}{5}$. Numerical evidence, to be given in Section 5, shows that for n higher still, MQ and IQ interpolants again diverge (when evaluated away from the parabola), whereas no case of divergence was seen for GA interpolants.

We conclude this section with a conjecture:

CONJECTURE 3.3. *Gaussian (GA) RBF interpolants will never diverge as $\varepsilon \to 0$.*

The strongest evidence in support of this conjecture comes from various experiments with the numerical algorithm that is described in Section 5.

4. Polynomial unisolvency, and some results for scattered points. An important concept in multivariate polynomial interpolation is unisolvency [1]. As we will see below, it also has some bearing on the RBF interpolation problem. The following theorem defines the concept and gives a necessary and sufficient condition.

THEOREM 4.1. *Let $\underline{x}_1$, $\underline{x}_2$, ... , $\underline{x}_n$ be n point locations, and let $p_1(\underline{x})$, $p_2(\underline{x})$, ..., $p_n(\underline{x})$ be n linearly independent polynomials. Then $\{\underline{x}_i\}$ is unisolvent with respect to $\{p_i\}$, i.e., there is a unique linear combination $\sum \beta_j p_j(\underline{x})$ which interpolates any data over the point set, if and only if $\det(P) \neq 0$, where*

$$P = \begin{bmatrix} p_1(\underline{x}_1) & p_2(\underline{x}_1) & \cdots & p_n(\underline{x}_1) \\ p_1(\underline{x}_2) & p_2(\underline{x}_2) & \cdots & p_n(\underline{x}_2) \\ \vdots & \vdots & & \vdots \\ p_1(\underline{x}_n) & p_2(\underline{x}_n) & \cdots & p_n(\underline{x}_n) \end{bmatrix} .$$

The proof follows trivially from linear algebra arguments. The application of the theorem is easy in 1-D. With $p_j(x) = x^{j-1}$ we get the Vandermonde matrix, which is non-singular as soon as none of the data points coincide. In more than one space dimension, it is less obvious how to best determine whether a point set is unisolvent or not. However, using randomly scattered data points promotes unisolvency. Any

1-D	2-D	3-D
$a_0 \neq 0$	$a_0 \neq 0$	$a_0 \neq 0$
$a_1 \neq 0$	$a_1 \neq 0$	$a_1 \neq 0$
$6a_0a_2 - a_1^2 \neq 0$	$a_2 \neq 0,\ 4a_0a_2 - a_1^2 \neq 0$	$a_2 \neq 0,\ 10a_0a_2 - 3a_1^2 \neq 0$
$5a_1a_3 - 2a_2^2 \neq 0$	$a_3 \neq 0,\ 9a_1a_3 - 4a_2^2 \neq 0$	$a_3 \neq 0,\ 21a_1a_3 - 10a_2^2 \neq 0$

TABLE 4.1
Conditions on the expansion coefficients.

regular features (such as the examples given in the previous section with points along a straight line or along a parabola) in a data set may lead to degeneration.

COROLLARY 4.2. *We can (also elementary) add that if* $\det(P) = 0$, *then the nullspace of* P *will describe all the possible ambiguities in the resulting interpolant of the specified form.*

We know from Theorem 2.2 that if $\lim_{\varepsilon \to 0} s(\underline{x})$ exists, it is a finite order polynomial. It was proved in [12] that in 1-D, we recover the lowest order interpolating polynomial (under some mild conditions on the expansion coefficients of the basis function, as briefly touched upon in Section 3). There are similar condition in more space dimensions. Table 4.1 gives the first four conditions in up to three space dimensions. Conditions of this type are needed for the proof of the theorem given below.

DEFINITION 4.3. *Let* P_K *be the set of all (multivariate) polynomials of degree* $\leq K$.

THEOREM 4.4. *If* $\{p_i\}$ *forms a basis for* P_K *and* $\{\underline{x}_i\}$ *is unisolvent with respect to* $\{p_i\}$, *then under some mild assumptions on the expansion coefficients of the radial basis function, the limiting RBF interpolant* $\lim_{\varepsilon \to 0} s(\underline{x})$ *is the unique interpolating polynomial of degree* $\leq K$ *to the given data.*

A proof and further discussion of the implications of the theorem can be found in [17] (an entirely different proof of the theorem can also be found in [19]). For now, we will only give a brief summary of some aspects relevant here. First of all, note that the number of data points must agree with the dimension of P_K for $\{p_i\}$ to be a basis. That is, in for example 2-D, $n = 1, 3, 6, 10, 15, 21, \ldots$ play a special role. If the unisolvency condition is not fulfilled, the interpolant may in the limit $\varepsilon \to 0$

- diverge,
- contain arbitrary elements from the nullspace of the matrix P,
- contain polynomial terms of higher degree than K.

EXAMPLE 4.5. *Interpolate* $f(x,y) = x - y - 2xy - 2y^2$ *at the six points* $\underline{x}_i = (x_i, y_i) = \{(0,0),\ (0,\frac{1}{2}),\ (0,1),\ (1,0),\ (1,\frac{1}{2}),\ (1,1)\}$ *with RBFs.* The natural choice of basis functions would be

$$p_1 = 1,$$
$$p_2 = x, \quad p_3 = y,$$
$$p_4 = x^2, \quad p_5 = xy, \quad p_6 = y^2.$$

This gives

$$P = \begin{bmatrix} 1 & 0 & 0 & 0 & 0 & 0 \\ 1 & 0 & \frac{1}{2} & 0 & 0 & \frac{1}{4} \\ 1 & 0 & 1 & 0 & 0 & 1 \\ 1 & 1 & 0 & 1 & 0 & 0 \\ 1 & 1 & \frac{1}{2} & 1 & \frac{1}{2} & \frac{1}{4} \\ 1 & 1 & 1 & 1 & 1 & 1 \end{bmatrix} .$$

This matrix is singular, and the nullspace of P is found to be $[0,\ 1,\ 0,\ -1,\ 0,\ 0]^T$. Therefore, the interpolant is undetermined with respect to any multiple of $1 \cdot p_2(\underline{x}) - 1 \cdot p_4(\underline{x}) = x - x^2 = x(1-x)$. If we try RBFs on this data set and let $\varepsilon \to 0$, we get

$$f(x,y) = x - y - 2xy - 2y^2 \qquad \text{original data}$$

IQ: $\frac{7}{5}x - y - \frac{2}{5}x^2 - 2xy - 2y^2$
MQ: $2x - y - x^2 - 2xy - 2y^2$
GA: $x - y - 2xy - 2y^2$ (recovers the original function)

We are getting different limits for all the three RBF types, but the differences are precisely of the type that was allowed to be undetermined according to the nullspace argument above. □

As shown in the examples from Section 3, with increasingly many points along a straight line or parabola, divergence of the IQ and MQ interpolants is preceeded by cases where the limiting interpolants are different. This result appears to be typical for many non-unisolvent cases. For example, if the points $(0, 1/4)$ and $(0, 3/4)$ are included in the above example, then both the IQ and MQ interpolants diverge like $O(\varepsilon^{-2})$ (the GA interpolant again converges to the original function).

5. Complex ε-plane considerations and the numerical Contour-Padé algorithm. The elements in the determinants in (2.3) are of size $O(1)$. Since expansions of the determinants for small ε typically start with some high power of ε, both matrices clearly become highly singular as $\varepsilon \to 0$. The matrix in the denominator is the same as the matrix A in (2.2). Thus, the coefficients λ_k must grow rapidly with decreasing ε. Since the sum in (2.1) is typically bounded, the sum must feature very severe cancellation of large quantities, and direct solution for $s(\underline{x})$ via (2.2) and (2.1) will be very ill conditioned. This heuristic argument can be made much more precise. In the case of scattered data, numerical evidence [17] strongly suggests the exponents that are shown in Table 5.1. These numbers are independent of the choice of MQ, IQ, or GA, and also hold for all other smooth RBFs that we have tested.

5.1. Numerical algorithm. The Contour-Padé algorithm in [14] is based on the fact that, in a complex ε-plane, the origin is a removable singularity (or, at worst, a low order pole) of the interpolant, which we now write as $s(\underline{x}, \varepsilon)$ in order to emphasize its dependence on ε. For a fixed $\underline{x}$, we compute $s(\underline{x}, \varepsilon)$ at equi-spaced ε-values around a circle centered at the origin in a complex ε-plane. Choosing the radius quite large, the direct approach using (2.2) and (2.1) works well. The next step is to take an FFT of these values. Some different cases will then arise:
  • All negative Fourier coefficients vanish: The positive ones then provide the coefficients in the Taylor expansion

$$s(\underline{x}, \varepsilon) = s_0(\underline{x}) + \varepsilon^2 s_2(\underline{x}) + \varepsilon^4 s_4(\underline{x}) + \dots \qquad (5.1)$$

	d - dimension	n - number of data points							
		2	3	5	10	20	50	100	200
Leading power of ε	1	2	6	20	90	380	2450	9900	39800
in both of the	2	2	4	12	40	130	570	1690	4940
determinants in (2.3)	3	2	4	10	30	90	360	980	2610
Leading inverse	1	2	4	8	18	38	98	198	398
power of ε in the	2	2	2	4	6	10	18	26	38
coefficients λ_k	3	2	2	4	4	6	10	14	18

TABLE 5.1

Powers of ε arising in cases of scattered data

This expansion is then well suited for numerical computation of $s(\underline{x}, \varepsilon)$ for small values of ε (including $\varepsilon = 0$, when it just reduces to its first coefficient).
- Some negative Fourier coefficients are present: With a Padé procedure, we can find all the poles of $s(\underline{x}, \varepsilon)$ inside the computational circle. If there is no pole at the origin, we can either again express the interpolant in the form (5.1) or, if we want the radius of convergence to extend out to the computational circle and not just to the nearest pole, we can represent the answer as a Taylor series together with a rational function in ε. If there is a pole right at the origin, the only difference compared to the previous cases is that (5.1) will need to also include some term(s) with negative powers of ε. For example, if the origin is a pole of order four, (5.1) would need to be replaced with

$$s(\underline{x}, \varepsilon) = \frac{1}{\varepsilon^4} s_{-4}(\underline{x}) + \frac{1}{\varepsilon^2} s_{-2}(\underline{x}) + s_0(\underline{x}) + \varepsilon^2 s_2(\underline{x}) + \varepsilon^4 s_4(\underline{x}) + \dots \quad . \quad (5.2)$$

Depending on what we are interested in, we can for example use the algorithm to generate
- The coefficients in (5.1) or in (5.2) (with an auxiliary rational function included, if desired).
- A display of the locations of the poles of $s(\underline{x}, \varepsilon)$ in the complex ε-plane. Since these originate from the A-matrix, they will be independent of $\underline{x}$ (they will depend only on $\phi(r)$ and on the data locations).

In the examples in Section 3, quite time consuming symbolic algebra (with *Mathematica*) was needed to obtain just the first one or two terms in (5.1) or (5.2) in cases of up to around $n = 5$ data points. In contrast, the numerical procedure gives, in seconds only, any number of expansion coefficients when n is up to around 100. Although this current size limit falls short of the sizes of some experimental data sets that one might want to use RBFs to analyze, the algorithm nevertheless vastly extends our ability to study phenomena related to $\varepsilon \to 0$ for RBF interpolants.

To illustrate this point, we use the Countor-Padé algorithm to compute the small ε expansion coefficients in (5.2) based on the 20 data points shown in Figure 5.1. As input data we use the cardinal function

$$f(x_j, y_j) = \begin{cases} 1 & \text{when } (x_j, y_j) = (-1, 0) \\ 0 & \text{otherwise} \end{cases} \quad .$$

Since each expansion coefficient is a function of $\underline{x}$, we can display the coefficients over some domain in $\underline{x}$-space. Figure 5.2 displays—across the triangle—the first six expansion functions $s_k(\underline{x})$, $k = -4, -2, 0, 2, 4, 6$, computed in the case of IQ RBFs. It
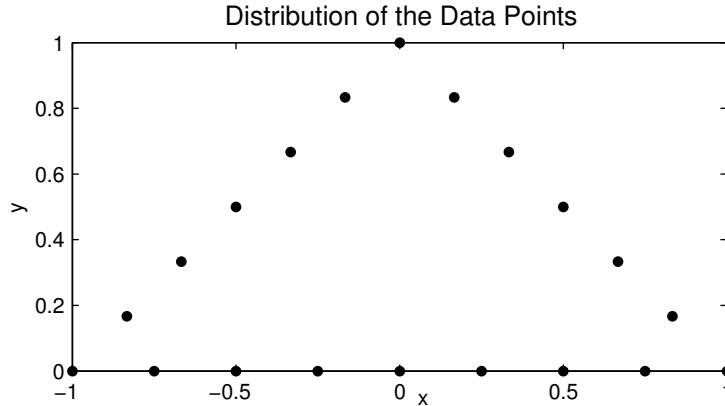
FIG. 5.1. *Distribution of the data points used for the example with computing expansion coefficients in Section 5.2.1 (The function value is one at the leftmost corner point, and zero at all the other points).*

transpires that this triangular distribution of data points produces a fourth order pole in the interpolant at $\varepsilon = 0$. The data points allow for this possibility since they clearly fail the polynomial unisolvency condition stated in Theorem 4.1 (the interpolating polynomial would be undetermined with respect to any multiple of $x(1 + x - y)(1 - x - y)$). In each of the subplots of Figure 5.2, solid circles mark where the data points are located. We see that $s_0(\underline{x})$ exactly matches the input cardinal data (and provides a good approximation to the data) whereas all other expansion functions are zero at the data point locations. Note the small scale on vertical axis for the $s_{-4}(\underline{x})$ and $s_{-2}(\underline{x})$ functions. This is consistent with the fact that we only see divergence in the interpolant for very small values of ε. When evaluating the interpolant on the boundary of the triangle, the $s_{-4}(\underline{x})$ and $s_{-2}(\underline{x})$ functions are equal to zero. This is similar to the example from Section 3.4 where 5 (or more) data points along a straight line cause divergence in the interpolant when evaluated off the line, but convergence when evaluated on the line. We also carried out the above experiment for the MQ and GA RBF. The interpolant based on MQ RBFs exhibits the same qualitative features as the one for the IQ case (for example, a fourth order pole at $\varepsilon = 0$). Like in all other cases that we have encountered, the interpolant based on GA RBFs has no pole at $\varepsilon = 0$; its expansion starts with the $s_0(\underline{x})$ term.

There are three options presently available for ensuring a convergent interpolant as $\varepsilon \to 0$:
  (a) In place of the RBF interpolant $s(\underline{x}, \varepsilon)$ use $s_0(\underline{x})$ (also possibly incorporating the additional finite-ε corrections given by $s_2(\underline{x})$, $s_4(\underline{x})$, etc.).
  (b) Avoid all data point distributions which are not consistent with the polynomial unisolvency requirements.
  (c) Use GA RBFs.
The first option is presently only available by means of the Countor-Padé algorithm, and testing data sets for dangerous point distributions does not appear to be practical. Assuming our Conjecture 3.3 is correct, the last option may be the most convenient one.

5.2. Pole locations in the complex ε-plane. Our discussion thus far has been on the occurrence (and non-occurrence) of a pole in $s(\underline{x}, \varepsilon)$ at $\varepsilon = 0$. We now focus
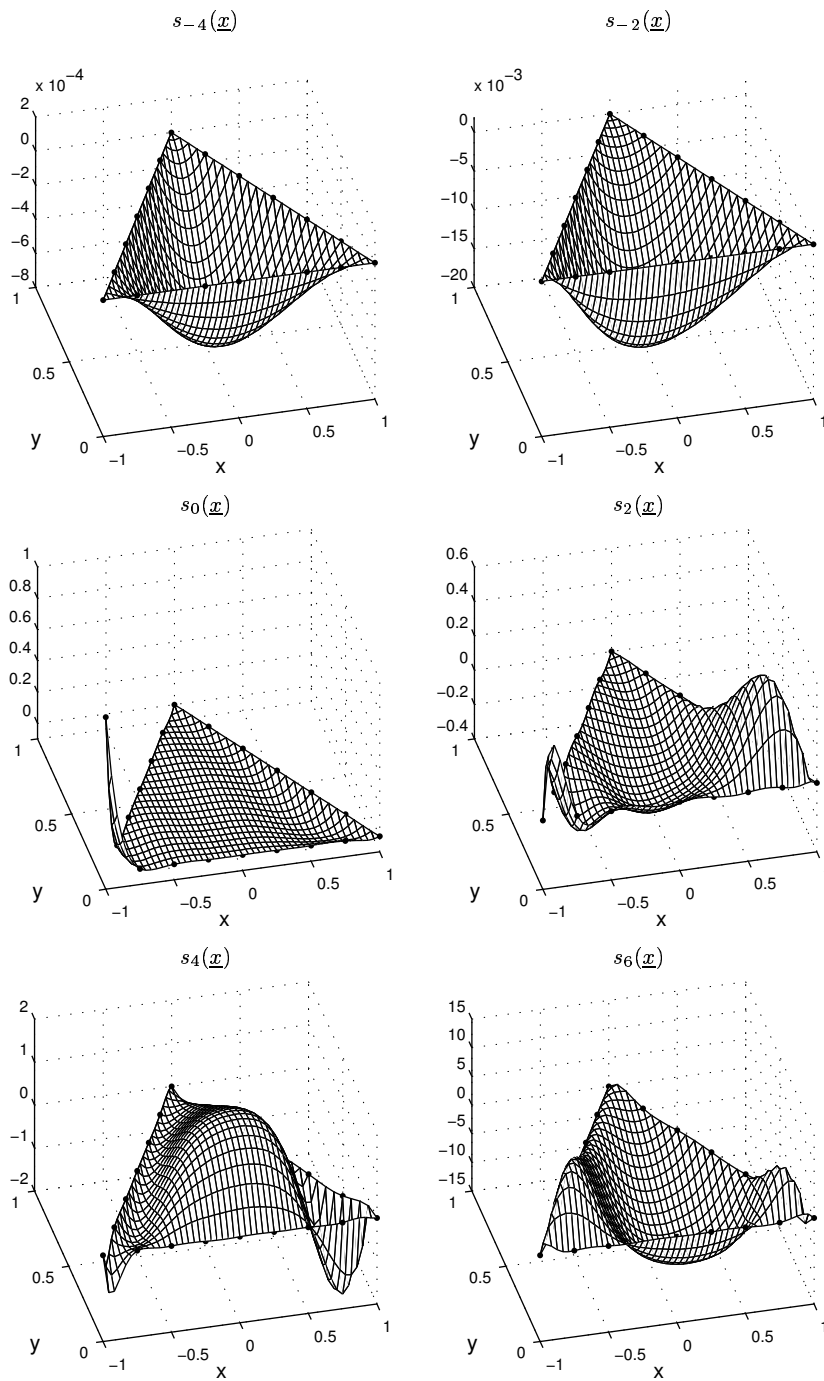
FIG. 5.2. *The first 6 terms from the expansion coefficients (5.2) of $s(\underline{x}, \varepsilon)$ for the example in Section 5.2.1. The solid circles mark the data points.*

on poles that arise in the complex ε-plane for different types of point distributions, and show how this lends additional insight to the $\varepsilon = 0$ pole phenomenon.

5.2.1. Points approach cases where polynomial unisolvency fails. As we have demonstrated, a pole at $\varepsilon = 0$ is directly related to failure of the unisolvency condition. Below we revisit a couple of the examples from Section 3 to see how the poles in the complex ε-plane behave as the points approach a non-unisolvent set.

Three points approach being collinear. Let the data points be at locations $\{(0, y_0), (\frac{1}{2}, 0), (1, 0)\}$ with cardinal data $\{1, 0, 0\}$. With MQ, the exact result $\varepsilon = \pm \frac{2\,i\,A}{a\,b\,c}$ noted above gives

$$\varepsilon_{1,2} = \pm \frac{2\,i\,y_0}{\sqrt{(1 + y_0^2)(1 + 4y_0^2)}} \ . \tag{5.3}$$

For small values of ε, we can alternatively expand the determinants in (2.3) to get

$$s(x, y, \varepsilon) = \frac{\frac{1}{4}y_0 y\, \varepsilon^4 + O(\varepsilon^6)}{\frac{1}{4}y_0^2\, \varepsilon^4 + \frac{1}{16}(1 - 2y_0^2)\, \varepsilon^6 + O(\varepsilon^8)} = \frac{y}{y_0} + O(\varepsilon^2). \tag{5.4}$$

When also y_0 is small, the first two terms in the denominator gives the approximate pole locations through

$$\frac{1}{4}y_0^2 + \frac{1}{16}\varepsilon^2 \approx 0 \quad \Rightarrow \quad \varepsilon_{1,2} \approx \pm\, 2iy_0 \ , \tag{5.5}$$

an excellent approximation to (5.3). Figure 5.3 (a) compares the approximation (5.5) to the exact (5.3) in the case of $y_0 = 0.01$. There is no visible discrepancy.

When the points approach being collinear (i.e. $y_0 \to 0$), the poles approach each other at the origin. When the points have become collinear, the ε^4-terms vanish from both the numerator and denominator in (5.4), and one can show that no poles remain.

Five points approach being collinear. Still considering MQ, we let now the point locations be $\{(0, y_0), (\frac{1}{4}, 0), (\frac{1}{2}, 0), (\frac{3}{4}, 0), (1, 0)\}$ with cardinal data $\{1, 0, 0, 0, 0\}$. For ε small, series expansion of the determinants gives

$$s(x, y, \varepsilon) = \frac{\frac{9\,y_0\,y}{1048576}\, \varepsilon^{14} + O(\varepsilon^{16})}{\frac{9\,y_0^2}{1048576}\, \varepsilon^{14} + O(\varepsilon^{16})} = \frac{y}{y_0} + O(\varepsilon^2).$$

In more detail, the denominator is

$$\det{}_{\text{den}} = \frac{1}{4294967296}[36864y_0^2\varepsilon^{14} \quad - \quad 2304(15 + 4y_0^2)y_0^2\varepsilon^{16} +$$
$$+ 288(85 + 50y_0^2 + 32y_0^4)y_0^2\varepsilon^{18} + \tag{5.6}$$
$$+ 9(63 - 1460y_0^2 - 1528y_0^4 - 2080y_0^6 - 1024y_0^8)\, \varepsilon^{20}] + O(\varepsilon^{22})$$

When ε is small, the terms for ε^{16} and ε^{18} will be small compared to the one for ε^{14}. The term for ε^{20} can be larger again (since it is lacking the factor y_0^2). The subsequent terms will again be decreasing. The determinant will therefore be zero also in the vicinity of the $\varepsilon-$values for which the terms with ε^{14} and ε^{20} add up to zero. This gives approximately

$$36864y_0^2 + 9 \cdot 63\varepsilon^6 \approx 0 \quad \Rightarrow \quad \varepsilon_k \approx \frac{4\,y_0^{1/3}}{\sqrt[6]{63}}\, e^{\frac{\pi\,i\,(2\,k-1)}{6}} \ , \quad k = 1, 2, \ldots, 6. \tag{5.7}$$
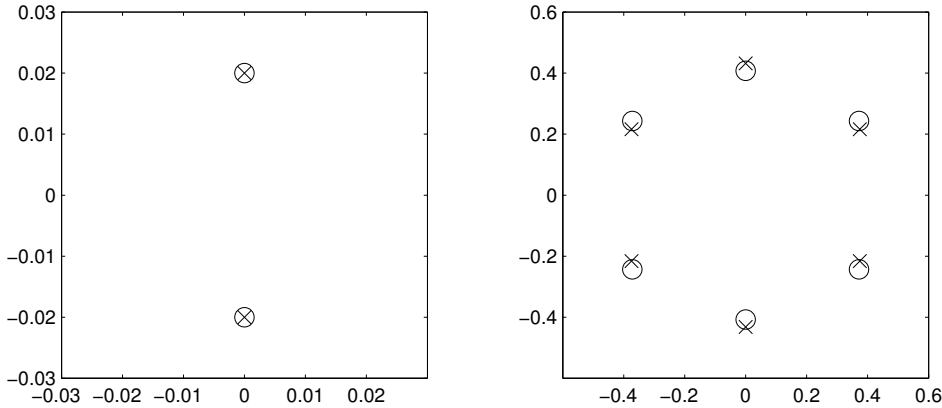
FIG. 5.3. *a and b. Exact and approximate locations of poles (circles and crosses, repsectively) when the data points approach being collinear: (a) three points, and (b) five points. The illustrations show the case of $y_0 = 0.01$.*

Part b of Figure 5.3 compares, again in the case of $y_0 = 0.01$, the numerically determined pole locations for $s(x, y, \varepsilon)$ against the values given by the approximation (5.7). The agreement is again good. It is clear from (5.7) that all the six poles move in to the origin as $y_0 \to 0$. When the data points have become collinear, we see from (5.6) that the ε^{14}, ε^{16} and ε^{18} terms vanish, leaving the denominator expansion to start with ε^{20}. In the numerator, it transpires that only the ε^{14} and ε^{16} terms vanish, leaving us with

$$s(x, y, \varepsilon) = \frac{\frac{27\, y^2}{134217728} \varepsilon^{18} + O(\varepsilon^{20})}{\frac{567}{4294967296} \varepsilon^{20} + O(\varepsilon^{22})} = \frac{32\, y^2}{21} \frac{1}{\varepsilon^2} + O(1),$$

i.e. divergence as $\varepsilon \to 0$ entirely in accordance with (3.3).

5.2.2. Points are located so that polynomial unisolvency fails. We consider again the case with points on a parabola that was studied analytically in Section 3.6, but focus here on the poles that arise in the complex ε-plane. It is too algebraically complex to give the pole locations in closed-form, so we determine them numerically using the Contour-Padé algorithm.

The n data points are located at $x_k = \frac{k-1}{n-1}$, $y_k = x_k^2$, $k = 1, 2, \ldots, n$. As soon as $n > 3$ the unisolvency condition fails. It was shown that for $n \geq 8$ there are cases where the interpolant diverges when using IQ or MQ. No divergent cases were found for GA (in accordance with our conjecture that GA interpolants never diverge as $\varepsilon \to 0$). Table 5.2 shows the number of poles inside the circle of radius 0.3 in the ε-plane and how many of those that are located at the origin (which leads to divergence). It is clear from the table that the GA RBF does behave differently from the other types of RBFs. We have not in any case observed poles at the origin for GA interpolants, and also the number of poles inside the fixed circle does not grow as fast. When n increases, it becomes more difficult to tell the exact number of poles, especially right at the origin. We have performed experiments for larger n that are not included here due to some numerical uncertainty in the precise numbers, but they seem to follow the same trends. The layout of the poles in the complex ε-plane for the different RBFs is shown in Figures 5.4–5.6.

	$|\varepsilon| \leq 0.3$			$\varepsilon = 0$		
n	MQ	IQ	GA	MQ	IQ	GA
4	0	0	0	0	0	0
5	2	2	2	0	0	0
6	4	4	0	0	0	0
7	4	8	2	0	0	0
8	6	10	4	2	2	0
9	10	10	2	2	2	0
10	14	14	4	2	2	0
11	16	20	4	2	2	0
12	20	24	4	4	4	0

TABLE 5.2

The number of poles within the circle $|\varepsilon| = 0.3$ and at $\varepsilon = 0$ for different RBFs
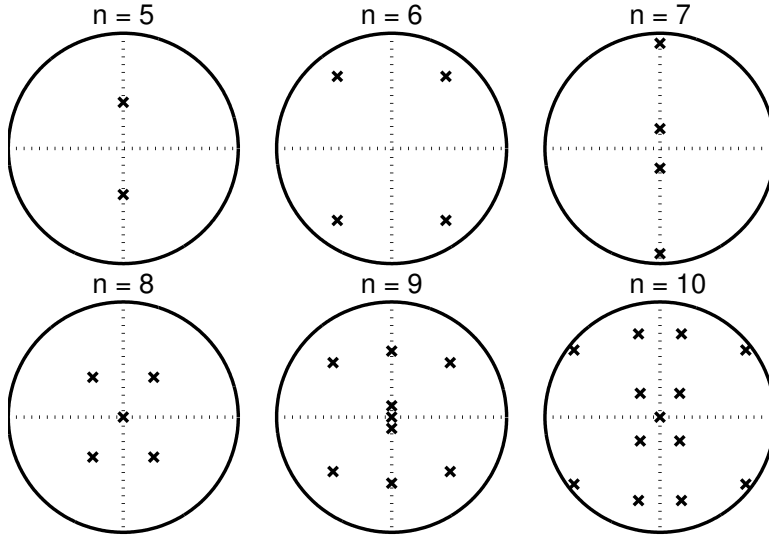
FIG. 5.4. *Pole locations inside the circle $|\varepsilon| = 0.3$ for points on a parabola using MQ*

5.2.3. Scattered points. It is only rarely possible to give all pole locations for $s(\underline{x}, \varepsilon)$ in closed-form. In the case of MQ with two arbitrarily located data points, the only poles appear at $\varepsilon = \pm \frac{\sqrt{2}\,i}{a}$ where a is the distance between the points. For three scattered points, we find similarly $\varepsilon = \pm \frac{2\,i\,A}{a\,b\,c}$ where A is the area of the triangle formed by the points, and a, b, c are the lengths of its sides.

For several scattered data points, we can again use the Contour-Padé algorithm to determine the location of the poles of the RBF interpolant. As an example, we consider the 45 randomly scattered data points shown in Figure 5.7 (a). Using the Contour-Padé algorithm, we find that this distribution of data points produces the poles for the MQ, IQ, and GA interpolants as shown in Figure 5.7 (b–d). The figure shows several properties that we have observed also for other scattered data point distributions:

- The poles for the IQ and MQ interpolants are usually close together, whereas, the location of the poles for the GA interpolant is usually quite different. For
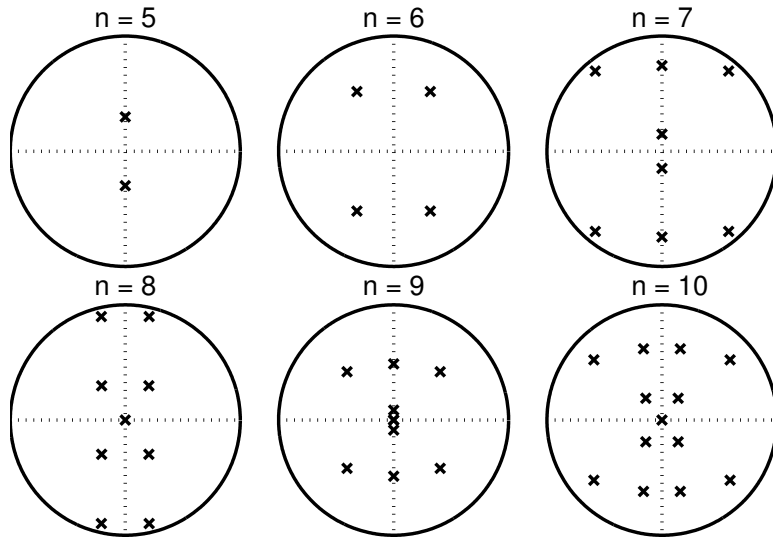
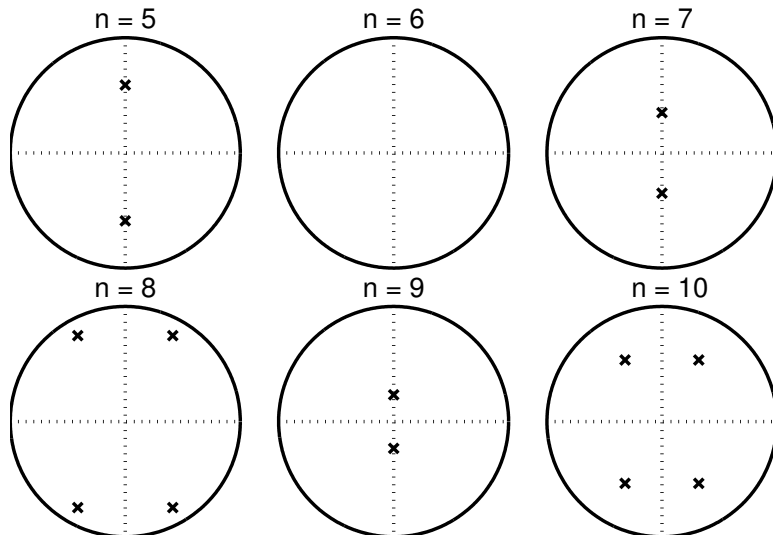FIG. 5.5. *Pole locations inside the circle $|\varepsilon| = 0.3$ for points on a parabola using IQ*

FIG. 5.6. *Pole locations inside the circle $|\varepsilon| = 0.3$ for points on a parabola using GA*

example, the GA interpolant does not in this case have any poles off the imaginary axis while both the IQ and MQ interpolants do.

• There tends to be only a few poles near the origin even for larger numbers of scattered data points. The figure shows that each of the interpolants only has two poles that are near $\varepsilon = 0$.

• We have never observed any poles at the origin, i.e. divergence in the interpolants, for any of the main types of smooth RBFs in the case of scattered data points.
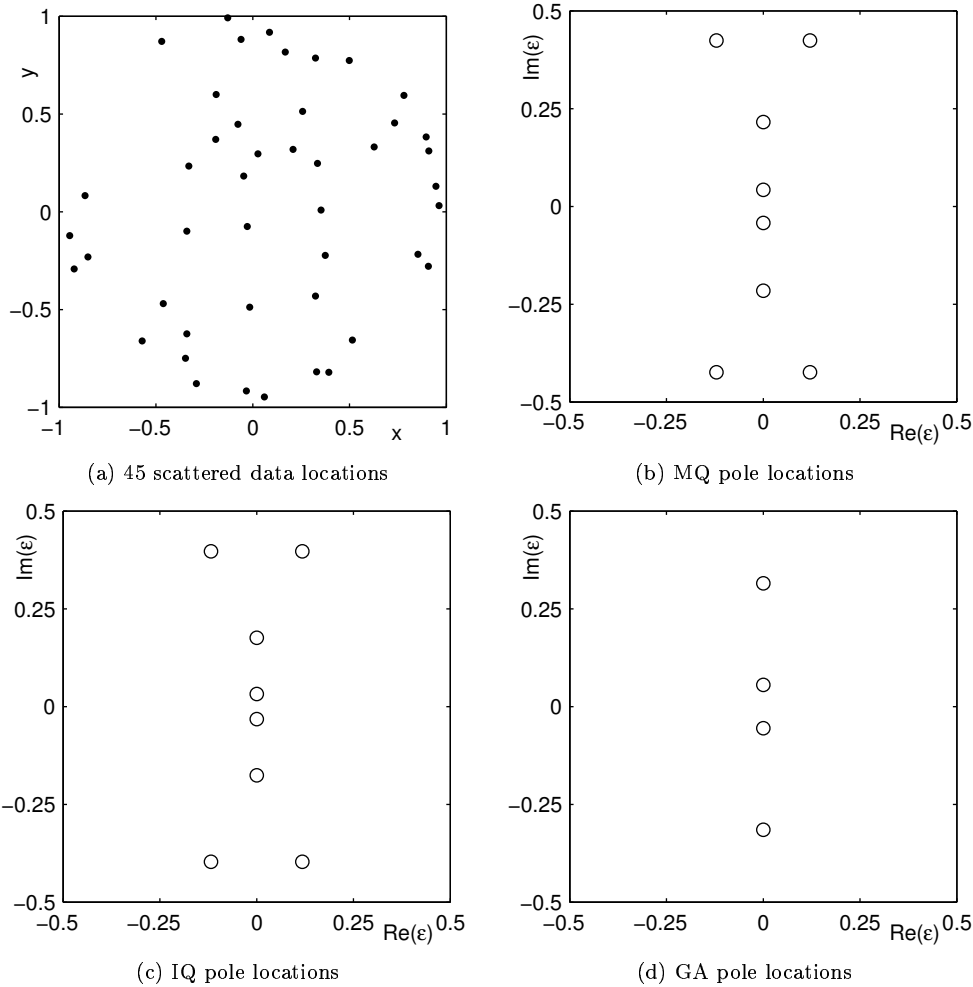
(a) 45 scattered data locations

(b) MQ pole locations

(c) IQ pole locations

(d) GA pole locations

FIG. 5.7. *a to d. (a) Location of the 45 randomly scattered data points across the unit circle. (b–d) Location of the poles of the RBF interpolant in cases of MQ, IQ, and GA respectively.*

6. RBF approximation with a constant term included. In place of (1.1), one can for example consider interpolants of the form

$$s(\underline{x}) = \alpha + \sum_{k=1}^{n} \lambda_k \phi(\|\underline{x} - \underline{x}_k\|) \tag{6.1}$$

together with the constraint $\sum_{k=1}^{N} \lambda_k = 0$. Reasons for considering this, and also more general extensions of this kind, can include

- Positive definiteness of the linear system to solve for the coefficients λ_k in (1.1) (for distinct points and non-zero ε) is guaranteed for GA and IQ, but only for MQ if we include a constant term together with the constraint above.
- On infinite Cartesian grids, MQ and IQ can (for non-zero ε) *exactly* reproduce polynomials up to degrees d and $d - 3$ (if $d \geq 3$) respectively, but GA cannot even reproduce a constant. Adding an explicit polynomial can provide such

a feature, in case that is desired.

- Adding polynomial terms can in some cases improve the accuracy of interpolants, especially near boundaries. This and other more effective boundary improving methods are discussed in [20].

In the limit of $\varepsilon \to 0$, polynomials (of degrees increasing with n) will be reproduced automatically, even in the case of scattered finite point sets, so the last two of the observations above may then be of less significance. Although more general extensions than (6.1) may be of interest, we here limit our study to this form. It transpires that most of the results in the previous sections carry over with little difference. For example, Theorem 2.1 now becomes:

THEOREM 6.1. *For cardinal data* $f_k = \left\{ \begin{array}{ll} 1 & if \ \ k=1 \\ 0 & otherwise \end{array} \right.$ *, the RBF interpolant of the form (6.1) becomes*

$$
s(\underline{x}) = \frac{\det \begin{bmatrix} \phi\left(\|\underline{x}-\underline{x}_1\|\right) & \phi\left(\|\underline{x}-\underline{x}_2\|\right) & \cdots & \phi\left(\|\underline{x}-\underline{x}_n\|\right) & 1 \\ \phi\left(\|\underline{x}_2-\underline{x}_1\|\right) & \phi\left(\|\underline{x}_2-\underline{x}_2\|\right) & \cdots & \phi\left(\|\underline{x}_2-\underline{x}_n\|\right) & 1 \\ \vdots & \vdots & \ddots & \vdots & \vdots \\ \phi\left(\|\underline{x}_n-\underline{x}_1\|\right) & \phi\left(\|\underline{x}_n-\underline{x}_2\|\right) & \cdots & \phi\left(\|\underline{x}_n-\underline{x}_n\|\right) & 1 \\ 1 & 1 & \cdots & 1 & 0 \end{bmatrix}}{\det \begin{bmatrix} \phi\left(\|\underline{x}_1-\underline{x}_1\|\right) & \phi\left(\|\underline{x}_1-\underline{x}_2\|\right) & \cdots & \phi\left(\|\underline{x}_1-\underline{x}_n\|\right) & 1 \\ \phi\left(\|\underline{x}_2-\underline{x}_1\|\right) & \phi\left(\|\underline{x}_2-\underline{x}_2\|\right) & \cdots & \phi\left(\|\underline{x}_2-\underline{x}_n\|\right) & 1 \\ \vdots & \vdots & \ddots & \vdots & \vdots \\ \phi\left(\|\underline{x}_n-\underline{x}_1\|\right) & \phi\left(\|\underline{x}_n-\underline{x}_2\|\right) & \cdots & \phi\left(\|\underline{x}_n-\underline{x}_n\|\right) & 1 \\ 1 & 1 & \cdots & 1 & 0 \end{bmatrix}} \quad (6.2)
$$

Both versions of the proof for Theorem 2.1 carry over, so we omit the details here.

Regarding the case with three data points along a straight line, equation (3.1) needs to be replaced with

$$
s(x,y) = \frac{(x-x_2)(x-x_3)}{(x_1-x_2)(x_1-x_3)} + \frac{1}{3} \cdot \frac{y^2}{(x_1-x_2)(x_1-x_3)} + O(\varepsilon^2)
$$

on the assumptions that $a_1 \neq 0$ and $a_2 \neq 0$. Similarly, for five points along a line, (3.3) needs to be replaced by

$$
s(x,y) = \frac{4\,y^2}{(x_1-x_2)(x_1-x_3)(x_1-x_4)(x_1-x_5)} \, \frac{a_2\,a_3}{(75\,a_3^2 - 140\,a_2 a_4)} \, \frac{1}{\varepsilon^2} \, + \, O(1),
$$

this time on the same assumption as for its earlier counterpart, viz. $2a_2^2 - 5a_1 a_3 \neq 0$. In this case, all the standard smooth RBF types (e.g. MQ, IQ, GA) lead to divergence. In the limit of $\varepsilon \to 0$, not only do the coefficients λ_k diverge to infinity, but so does the constant α in (6.1). Although the limiting interpolant along a line of data points will again become the Lagrange interpolation polynomial, there is no immediate counterpart to Theorem 3.1.

7. Conclusions. We have in this study been considering interpolants based on smooth RBFs featuring a shape parameter ε. It has been known for a long time that $\varepsilon > 0$ leads to a well-defined interpolant in the case of Gaussian RBFs and, thanks to more recent work of Micchelli [2] and others, equivalent results are known for many other cases. In this study, we are making a number of observations regarding the limit when the basis functions become increasingly flat ($\varepsilon \to 0$). We first note

- When the limit exists, it takes the form of a multivariate polynomial,
- The Contour-Padé algorithm permits numerical computations—without any deterioration of the conditioning—all the way down to the $\varepsilon \to 0$ limit.

We then make a number of observations that shed new light on this limit. In particular, we note that

- The existence of the limit, for most RBFs, depends very critically on the data point distributions. This is connected to the issue of 'polynomial unisolvency'.
- Gaussian RBFs appear to have the remarkable property of never leading to a divergent interpolant as $\varepsilon \to 0$. At least among other standard types of smooth RBFs, Gaussians are unique in this respect.

REFERENCES

[1] R. J. Y. McLeod and M. L. Baart. *Geometry and Interpolation of Curves and Surfaces.* Cambridge University Press, Cambridge, 1998.

[2] C. A. Micchelli. Interpolation of scattered data: distance matrices and conditionally positive definite functions. *Constr. Approx.*, 2:11–22, 1986.

[3] E. W. Cheney and W. A. Light. *A Course in Approximation Theory.* Brooks/Cole, New York, 2000.

[4] M. J. D. Powell. The theory of radial basis function approximation in 1990. In W. Light, editor, *Advances in Numerical Analysis, Vol. II: Wavelets, Subdivision Algorithms and Radial Functions*, pages 105–210. Oxford University Press, Oxford, UK, 1992.

[5] Z. Wu and R. Schaback. Local error estimates for radial basis function interpolation of scattered data. *I.M.A. J. Numer. Anal.*, 13:13–27, 1993.

[6] W. R. Madych and S. A. Nelson. Bounds on multivariate polynomials and exponential error estimates for multiquadric interpolation. *J. Approx. Theory*, 70:94–114, 1992.

[7] R. Schaback. Error estimates and condition numbers for radial basis function interpolants. *Adv. Comput. Math.*, 3:251–264, 1995.

[8] J. Yoon. Spectral approximation orders of radial basis function interpolation on the Sobolev space. *SIAM J. Math. Anal.*, 23(4):946–958, 2001.

[9] R. E. Carlson and T. A. Foley. The parameter R^2 in multiquadric interpolation. *Comput. Math. Appl.*, 21:29–42, 1991.

[10] T. A. Foley. Near optimal parameter selection for multiquadric interpolation. *J. Appl. Sci. Comput.*, 1:54–69, 1994.

[11] S. Rippa. An algorithm for selecting a good value for the parameter c in radial basis function interpolation. *Adv. Comput. Math.*, 11:193–210, 1999.

[12] T. A. Driscoll and B. Fornberg. Interpolation in the limit of increasingly flat radial basis functions. *Comput. Math. Appl.*, 43:413–422, 2002.

[13] B. Fornberg. *A Practical Guide to Pseudospectral Methods.* Cambridge University Press, Cambridge, 1996.

[14] B. Fornberg and G. Wright. Stable computation of multiquadric interpolants for all values of the shape parameter. *Comput. Math. Appl.*, 2003. Submitted.

[15] E. Larsson and B. Fornberg. A numerical study of some radial basis function based solution methods for elliptic PDEs. *Comput. Math. Appl.*, 2001. To appear.

[16] M. J. D. Powell. Radial basis function methods for interpolation to functions of many variables. DAMTP Report NA11, University of Cambridge, 2001.

[17] E. Larsson and B. Fornberg. Theoretical aspects of multivariate interpolation with increasingly flat radial basis functions. To be submitted.

[18] B. Fornberg and N. Flyer. Accuracy of radial basis function derivative approximations in 1-d. *Adv. Comput. Math.*, 2003. Submitted.

[19] R. Schaback. Multivariate interpolation by polynomials and radial basis functions. Submitted, 2002.

[20] B. Fornberg, T. A. Driscoll, G. Wright, and R. Charles. Observations on the behavior of radial basis functions near boundaries. *Comput. Math. Appl.*, 43:473–490, 2002.